IEEE Photonics Journal
An IEEE Photonics Society Publication

Open Access

Fiber-to-Fiber Optical Switching Based on Gigantic Bloch-Surface-Wave-Induced Goos–Hanchen Shifts

Volume 5, Number 1, February 2013

Yuhang Wan
Zheng Zheng
Weijing Kong
Xin Zhao
Jiansheng Liu

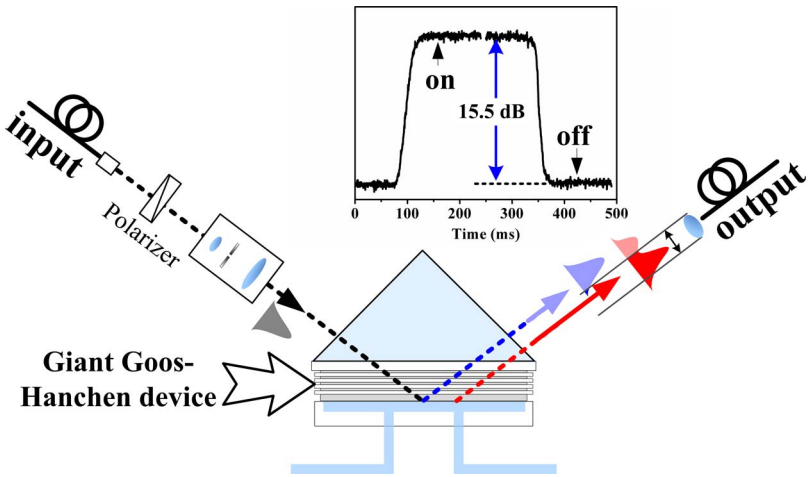

DOI: 10.1109/JPHOT.2012.2234734
1943-0655/$31.00 ©2012 IEEE

IEEE photonics SOCIETY

IEEE

Fiber-to-Fiber Optical Switching Based on Gigantic Bloch-Surface-Wave-Induced Goos–Hanchen Shifts

Yuhang Wan, Zheng Zheng, Weijing Kong, Xin Zhao, and Jiansheng Liu

School of Electronic and Information Engineering, Beihang University, Beijing 100191, China

DOI: 10.1109/JPHOT.2012.2234734
1943-0655/$31.00 ©2012 IEEE

Manuscript received October 28, 2012; revised December 9, 2012; accepted December 10, 2012. Date of publication December 20, 2012; date of current version February 6, 2013. This work was supported in part by the 973 Programs 2009CB930701 and 2012CB315601 and in part by the NSFC under Grants 60921001 and 61205078. Corresponding author: Z. Zheng (e-mail: zhengzheng@buaa.edu.cn).

Abstract: Fiber-to-fiber on–off optical switching based on the gigantic Goos–Hanchen (GH) shift on an optical beam induced by the Bloch surface wave is experimentally demonstrated for the first time. Through changing the refractive index of the cladding covering a truncated 1-D photonic crystal, the enhanced GH shift can be toggled dynamically from zero to submillimeter range. By using the finite coupling aperture of the fiber and selecting an optimized pass region of the beam to the output fiber, high extinction ratio can be achieved with reasonable insertion loss. It is also demonstrated that a refractive index change of $< 2^{*}10^{-3}$ is sufficient to realize the switching, which opens the way to realize faster and more compact integrated GH switches.

Index Terms: Optical switch, Goos–Hanchen (GH) effect, Bloch surface wave (BSW).

1. Introduction

With the development of the optical communication technologies at an astounding pace in the past half of century, being dynamic and reconfigurable has become one of the essential features of current optical fiber networks [1]–[3]. Various optical switches that can dynamically turn on and off optical signals in their paths have become an integral part of these networks [4]. As the studies on optical switching devices become an important topic in photonic research, different physical mechanisms and device structures, including optical microelectromechanical systems (MEMS) and devices based on thermal-optic, electro-optic, or acousto-optic effects, have been explored to meet the demands of fiber-optic systems.

Among the studied fiber-optic compatible schemes, most of them could fall into two main categories: those based on interferometric configurations that convert an applied phase changes to a change in the transmission of the device and those based on directly shifting the beam position so that it may or may not couple into a fiber. The interferometric scheme can be readily implemented with waveguide-based devices [3]. The phenomena like thermal-optic and electro-optic effects can be utilized to change the refractive index of the waveguide material, e.g., the phase delay of the signal passing through the waveguide. The waveguide-based switches can be very compact and easy to be integrated with fibers, even though their costs are usually relatively higher.

The opto-mechanical (OM) switches, on the other hand, operate by simply directing the beam towards or away from the coupling waveguide/fiber to switch the light on or off. In those implementations using bulk optics, mechanical moving parts are used to change the direction or the position of the coupling fiber or other optical components in the beam path, such as prism, lens,

mirror, and so on. The concept of the OM switches is very simple and has been widely adopted since the early stage of the development of optical switches. High extinction ratio can be achieved with such devices, but they are relatively bulky and the switching speed is also limited. Due to the emerging of microfabrication technologies, the MEMS-based switching technology becomes an attractive and feasible solution with greatly reduced device size and power consumption. Some innovative approaches had also been explored to change the beam path without moving parts. Total internal reflection (TIR) is a simple but effective effect that has been used in such schemes. One impressive example was the 2-D switch fabricated by Agilent, where a liquid bubble can be created and removed at the cross intersection of two special waveguides [5]. With the presence of the bubble, the light undergoes TIR and its path is bent 90° and routed into the other waveguide. Another example is the oil latching interfacial tension variation effect (OLIVE) switch, where a pair of microheaters are used to control the movement of an air bubble in a silica slit [6]. When the cross point of the transmission and the reflection path is filled with the refractive index matching oil, the light passes through directly. When it is filled with the air bubble, the light is reflected due to the total internal reflection at the sidewall of the slit.

Other optical phenomena associated with TIR or similar effects could also be leveraged to realize novel optical switching schemes. Goos–Hanchen (GH) effect is one of the well-known nonspecular phenomena caused by the reflection of a finite-sized beam from a planar surface. The GH effect refers to the lateral shift of the reflected beam from its expected geometric position under reflection. While the GH shift (GHS) is usually only on the order of wavelength and hardly observable under most common optical setups, it has been widely studied after it was first discovered experimentally in 1947 [7]. The feasibility of extending an OLIVE switch to a 2×2 optical waveguide switch by utilizing the GH effect has been studied [8]. However, as the GHS realized in that device was only around a couple of microns, demonstration of the optical switching capability was not yet carried out. Methods to enhance the GH effect with more complicated optical structure or materials with special optical characteristics have been intensively investigated theoretically in the past few years with fewer experimental verifications [9]–[12]. It is recently demonstrated that the generation of giantly enhanced GHS on the order of hundreds of times of wavelength can be achieved using a relatively simple structure [13]–[15]. Both the guided and surface wave excited in a truncated 1-D photonic band gap (PBG) structure are shown to significantly boost the GH effect with relatively low optical losses. The giant GHS is also observed to be highly sensitive to the excitation condition of the Bloch surface wave (BSW), which opens the possibility to actively control this phenomenon [14], [16].

Here, we propose and experimentally demonstrate a 1×1 optical switching scheme based on the giant GH effect. Through tuning the refractive index of the cladding over a device based on the Bloch-surface-wave-Induced Giant GH (BIGG) effect high extinction ratio, fiber-to-fiber optical switching is demonstrated with an ATR configuration. This could be, as far as we know, the first GH-effect-based optical switching scheme ever realized.

2. Principle of Operation and Experimental Setup

The schematic of the fiber-to-fiber optical switching setup is shown in Fig. 1. The fiber output from a laser source is collimated and spatial-filtered to generate a Gaussian beam. The beam has a radius of $\sim$750 μm at its waist, and its state of polarization is set to be p-polarized by a polarizer and a polarization controller is placed before that to control the power of the beam incident. The beam is incident onto the giant GH device through a high-refractive-index glass prism (SF10, $n = 1.704$) and is reflected. The reflected beam is focused by a lens $(f = 10\ \text{mm})$ and coupled back into a piece of fiber. The position of the coupling lens and the output fiber are laterally tuned so that the coupling of the beam into the fiber without the GH effect is minimized. Their position, instead, is around the beam path when maximal GHS is observed. By leveraging the limited numerical aperture (NA) and the corresponding coupling aperture of the fiber, only when the GHS is significantly enhanced can a large portion of the beam be coupled into the fiber, corresponding to the "on" state of the switch. When the GH effect is reduced, the beam shifts out of this aperture so that the light is not coupled into the fiber, i.e. the output is switched off.

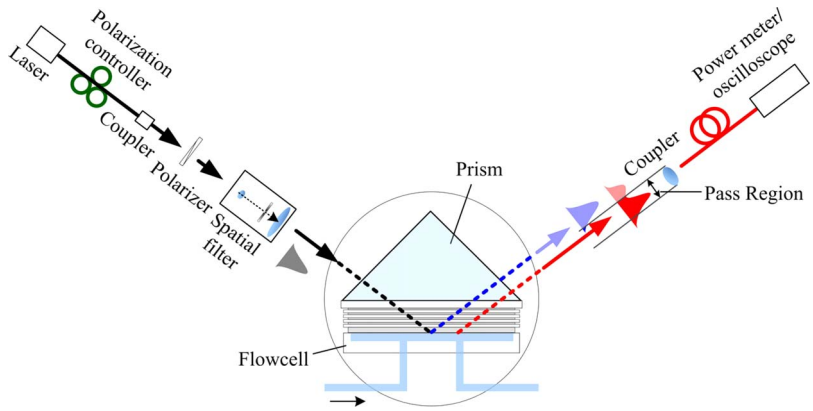

Fig. 1. Schematic of the experimental setup.

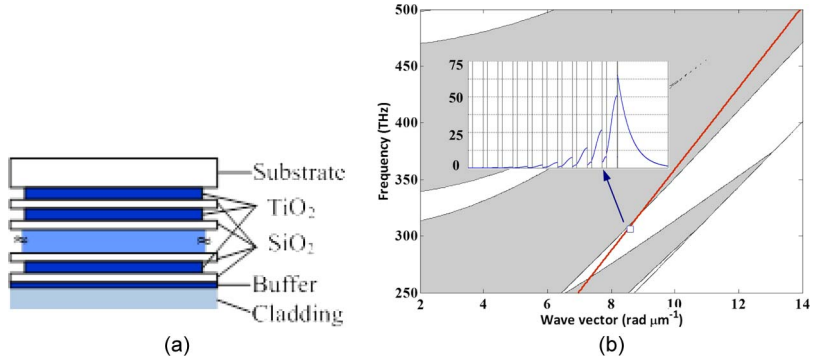

Fig. 2. (a) Schematic of the BIGG device; (b) dispersion diagram of frequency versus wave vector of the BIGG device for the P polarization light.

The structure of the BIGG device is shown in Fig. 2(a). The device consists of specially designed ten periods of alternating TiO_2 $(n = 2.30)$ and SiO_2 $(n = 1.434)$ layers on a ZF10 glass slide $(n = 1.668)$, terminated with a TiO_2 buffer layer [13]. The thicknesses of the TiO_2 layer and SiO_2 layer of the periodic layers, and the buffer layer are 163 nm, 391 nm, and 23 nm, respectively. In Fig. 2(b), the dispersion diagram of frequency verses wave vector for p-polarization is shown. The device is designed to be able to excite BSW when the refractive index of the cladding is 1.33, i.e., the device is covered by water, at the 980-nm wavelength. The surface mode excited for water as the cladding is plotted, as well as the field distribution of the BSW mode. We note that the cladding is designed with the aqueous materials so that their refractive indices can be easily tuned by changing to different liquids with different indices.

To facilitate the delivery of different liquids to the surface of the BIGG device, a PDMS flow cell is attached to the other side of the GH device, and the injection procedure is controlled by a homemade microfluidic control system. By flowing liquids with different indices that change the refractive index of the cladding medium over the device, the GH effect can be turned on or off, which in turn toggles the switch.

While, during the demonstration of the switching operation, the incident angle of the beam is fixed at that of the maximum GHS with water, for characterizing the fabricated device, the incident angle can be scanned by a high-resolution step-motor rotation stage when the angular-dependent GHS is measured. The GHS can be accurately measured by capturing the reflected beam spots by a CCD camera as the incident angle changes. For the captured image of the reflected beam, the position of the reflected beam is defined as the centroid of the horizontal intensity distribution,

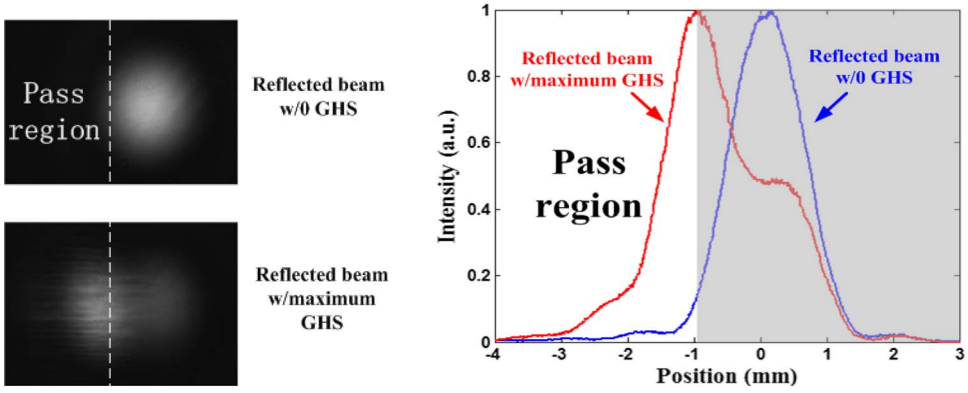

Fig. 3. (a) The reflected beam profiles captured by the CCD camera; (b) the corresponding intensity distributions.

where the horizontal intensity distribution is obtained by averaging a horizontal strip with a height of 30% of the 1/e intensity radius around the vertical center of the beam captured. To measure the GHS, the reflected beam spots obtained by injecting air into the flow cell or of the s-polarization are taken as the reference, since the GHS is expected to be negligible for those circumstances within the angular range of interest.

3. Results and Discussions

First, the GH characteristics of the BIGG device are characterized. As shown in [14], under the condition of exciting the BSW, i.e., at the incident angle of 53.44°, the GH effect is significantly enhanced and a peak value of ~740 μm can be obtained. The reflected beam intensity profiles captured by a CCD camera with and without the BIGG effect are shown in Fig. 3(a), where the intensity distributions along the horizontal direction are plotted in Fig. 3(b). Compared with the original beam shape, a major portion of the reflected beam shifted away from where it is supposed to be at the maximal GHS. The shifted beam profile has a shifted peak significantly away from the original one. Yet, as commonly seen by the enhanced giant GH effects demonstrated [14], [17], the tail of the profile still has overlap with the unshifted beam position. Through properly selecting a pass region and selectively collecting the light in that region into the output fiber, while rejecting that in the other region, a good switching extinction ratio is expected. Because of the remaining overlap in the two beam profiles, moving the boundary of the pass region further to the left would result in an improved extinction ratio at the price of reduced collection efficiency of the "on" state. Yet, our later results show that with the giant GHS high extinction ratio can be achieved under acceptable insertion loss.

To test the performance of the GH effect based optical switch, water and air are injected into the flow cell, respectively, and the reflected light coupled into the fiber is measured by an optical power meter (Newport 840). The input beam before the prism is measured to be 716 μw. After coupling into the output fiber, the output powers are measured to be 2.86 μw and 102 μw for air and water, respectively, which correspond to the "off" and "on" states, respectively. Therefore, an extinction ratio of 1 : 35.6 is achieved with an insertion loss of 8 dB.

In order to analyze the effect of GHS on the switching performance, the optical powers in the system are further measured. It is found that the reflected beams after the prism are measured to be 609 μw and 420 μw for air and water, respectively. Compared with the input power, the loss of the beam when air is injected, i.e. without the GH effect, is mainly due to the reflection losses of the beam entering and exiting the uncoated prism (estimated to be ~6%/surface), as the incident angle is beyond the critical angle for total internal reflection. We note that this loss can be reduced by the use of antireflection coating in the future. The reduction in the reflected power under the GH effect is

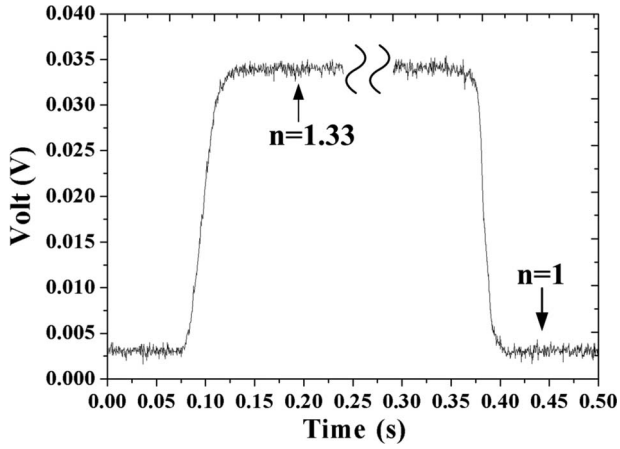

Fig. 4. Recorded oscilloscope trace when changing the cladding materials.

due to the optical loss associated with the excitation of BSW. The interfacial scattering loss and material absorption of the device structure are the major sources of this loss [13], which could be further reduced by improving the fabrication process. Besides the reflection loss, the loss induced by the coupling from free space back to the fiber contributes much to the overall insertion loss. Currently, we have achieved the minimal coupling loss of $\sim$3 dB using the coupling lens. Therefore, the extra loss of the proposed switching scheme due to the selection of the passing region accounts for only $\sim$2–3 dB within the total loss budget.

Dynamic switching capability of this GHS-based optical switch is preliminarily demonstrated by quickly injecting water into and removing it from the flow cell. As shown in Fig. 4, a Si photodiode connected to a real-time oscilloscope (Rigol, DS1102C) is used to measure the optical output from the fiber. We note that the baseline shown ($\sim$3 mV) is a background signal due to the dark current from the photodiode and has little to do with the actual contrast ratio that had been measured above. As seen in the figure, it takes about 40 ms to turn "on" or turn "off" this optical switch, when the flow rate is 50 μl/s limited by the microfluidic control system. By further increasing the flow rate or reducing the volume of the flow cell, the switching time could be further shortened.

Due to the various challenges in handling and controlling fluids in a switching device, we aim to realize switching with a much smaller change in the refractive index so that other schemes of index tuning could be adopted. Because of the high sensitivity of the excitation of the BSW to the refractive index of the cladding, it is expected that very small change in the refractive index of the cladding material could cause obvious difference of the induced GHS [14]. Therefore, instead of air, 1% NaCl solution is used to replace the air to switch "off" the GH effect and the switch. The saline solution has a refractive index difference of $1.76^{*}10^{-3}$ RIU from pure water, where the GHS is maximized. Thus, as shown in Fig. 5, the injection of the saline solution effectively turned off the output, in contrast to the result for pure water. Again, we note that the baseline in Fig. 5 is due to the dark signal of the photodetection circuit. Thus, it is demonstrated that a refractive index change $< 2^{*}10^{-3}$ RIU is sufficient to operate this BSW-induced-GH-shift based optical switch.

We note that, in the current experimental setup, the switching scheme is carried out by changing the bulk medium in the fluidic channel using mechanical pumps, and the switching speed is determined by the time filling the flow cell with a different medium. Instead, novel microfluidic techniques, e.g., the electrowetting-driven scheme [18], can be applied to control the movements of the liquids over the surface of the switch device without the bulky and power-consuming pumps. On the other hand, as the required refractive index change ($\sim 10^{-3}$ RIU) for switching is relatively small, those effects such as the thermo-optic effects can also be leveraged, which can greatly improve the speed and compactness of the device.

It is also noted that, since the GH effect is polarization dependent, the switching experiments discussed here are carried out for the p-polarized input, while the s-polarized light would experience

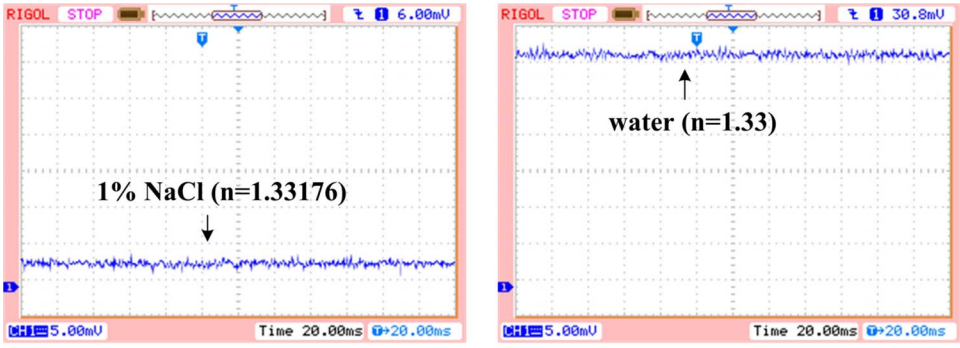

(a) (b)

Fig. 5. Output signal of (a) the "Off" state with 1%NaCl; (b) "On" state with pure water.

no GHS. The polarization dependence of the device could enable the development of additional polarization-related functionalities in the future, e.g., the polarization splitting device.

The current experiments are carried out at 980-nm wavelength, the proposed BIGG structure and the switching mechanism can be readily designed and realized to operate at different wavelengths as well, such as the more important 1550-nm wavelength.

4. Conclusion

A reflection-type optical switch based on the Bloch-surface-wave-induced GH effect has been experimentally demonstrated, enabled by the gigantic submillimeter GHS. This is, to our knowledge, the first successful experimental demonstration of such a scheme based on the GH effect. An extinction ratio of 1 : 35.6 has been achieved with a switching time of $\sim$40 ms in a microfluidic system. The reflection type of geometry of our demonstrated scheme could facilitate the further development of arrayed switching configurations with multiple parallel inputs and outputs. Boosted by the giant increase in the magnitude of the achievable GHS, it is expected that this interesting yet so far less utilized effect could come into play in more and more practical applications in the future.

References

[1] J. Berthold, A. A. M. Saleh, L. Blair, and J. M. Simmons, "Optical networking: Past, present, and future," *J. Lightw. Technol.*, vol. 26, no. 9, pp. 1104–1118, May 2008.
[2] M. J. O'Mahony, D. Simeonidou, D. K. Hunter, and A. Tzanakaki, "The application of optical packet switching in future communication networks," *IEEE Commun. Mag.*, vol. 39, no. 3, pp. 128–135, Mar. 2001.
[3] G. I. Papadimitriou, C. Papazoglou, and A. S. Pomportsis, "Optical switching: Switch fabrics, techniques, and architectures," *J. Lightw. Technol.*, vol. 21, no. 2, pp. 384–405, Feb. 2003.
[4] N. A. Jackman, S. H. Patel, B. P. Mikkelsen, and S. K. Korotky, "Optical cross connects for optical networking," *Bell Labs Tech. J.*, vol. 4, no. 1, pp. 262–281, Jan.–Mar. 1999.
[5] S. Venkatesh, R. Haven, D. Chen, H. L. Reynolds, G. Harkins, S. Close, M. Troll, J. E. Fouquet, D. Schroeder, and P. McGuire, "Recent advances in bubble-actuated cross-connect switches," in *Proc. Cleo(R)/Pac. Rim*, 2001, vol. 1, pp. 414–415.
[6] M. Makihara, N. Sato, F. Shimokawa, and Y. Nishida, "Micromechanical optical switches based on thermocapillary integrated in waveguide substrate," *J. Lightw. Technol.*, vol. 17, no. 1, pp. 14–18, Jan. 1999.
[7] F. Goos and H. Hanchen, "Ein neuer und fundamentaler Versuch zur Totalreflexion," *Ann. Phys. (Leipzig)*, vol. 436, no. 7/8, pp. 333–346, 1947.
[8] T. Sakata, H. Togo, and F. Shimokawa, "Reflection-type 2$\times$ 2 optical waveguide switch using the Goos–Hanchen shift effect," *Appl. Phys. Lett.*, vol. 76, no. 20, pp. 2841–2843, May 2000.
[9] H. Gilles, S. Girard, and J. Hamel, "Simple technique for measuring the Goos–Hanchen effect with polarization modulation and a position-sensitive detector," *Opt. Lett.*, vol. 27, no. 16, pp. 1421–1423, Aug. 2002.
[10] F. Pillon, H. Gilles, and S. Girard, "Experimental observation of the Imbert–Fedorov transverse displacement after a single total reflection," *Appl. Opt.*, vol. 43, no. 9, pp. 1863–1869, Mar. 2004.
[11] X. Yin, L. Hesselink, Z. Liu, N. Fang, and X. Zhang, "Large positive and negative lateral optical beam displacements due to surface plasmon resonance," *Appl. Phys. Lett.*, vol. 85, no. 3, pp. 372–374, Jul. 2004.

[12] M. Merano, A. Aiello, G. W. t Hooft, M. P. van Exter, E. R. Eliel, and J. P. Woerdman, "Observation of Goos–Hanchen shifts in metallic reflection," *Opt. Exp.*, vol. 15, no. 24, pp. 15 928–15 934, Nov. 2007.
[13] Y. Wan, Z. Zheng, W. Kong, Y. Liu, Z. Lu, and Y. Bian, "Direct experimental observation of giant Goos–Hänchen shifts from bandgap-enhanced total internal reflection," *Opt. Lett.*, vol. 36, no. 18, pp. 3539–3541, Sep. 2011.
[14] Y. Wan, Z. Zheng, W. Kong, X. Zhao, Y. Liu, Y. Bian, and J. Liu, "Nearly three orders of magnitude enhancement of Goos–Hanchen shift by exciting Bloch surface wave," *Opt. Exp.*, vol. 20, no. 8, pp. 8998–9003, Apr. 2012.
[15] I. V. Soboleva, V. V. Moskalenko, and A. A. Fedyanin, "Giant Goos-Hänchen effect and Fano resonance at photonic crystal surfaces," *Phys. Rev. Lett.*, vol. 108, no. 12, pp. 123901-1–123901-5, Mar. 2012.
[16] W. Kong, Y. Wan, and Z. Zheng, "Highly-sensitive, Bloch-surface-wave induced Giant Goos–Hanchen shift sensing," presented at the Proc. Lasers Electro-Opt. Quantum Electron. Laser Sci. Conf., San Jose, CA, 2012, CTh4L.6.
[17] I. V. Shadrivov, A. A. Zharov, and Y. S. Kivshar, "Giant Goos–Hanchen effect at the reflection from left-handed metamaterials," *Appl. Phys. Lett.*, vol. 83, no. 13, pp. 2713–2715, Sep. 2003.
[18] J. T. Cheng and C. L. Chen, "Active thermal management of on-chip hot spots using EWOD-driven droplet microfluidics," *Exp. Fluids*, vol. 49, no. 6, pp. 1349–1357, Dec. 2010.